Non-Peptide Angiotensin II Receptor Antagonists: Chemical Feature Based Pharmacophore Identification

Eva M. Krovat† and Thierry Langer*

Department of Pharmaceutical Chemistry, Institute of Pharmacy, University of Innsbruck, Innrain 52a, A-6020 Innsbruck, Austria

Received August 30, 2002

Chemical feature based pharmacophore models were elaborated for angiotensin II receptor subtype 1 (AT_1) antagonists using both a quantitative and a qualitative approach (Catalyst HypoGen and HipHop algorithms, respectively). The training sets for quantitative model generation consisted of 25 selective AT_1 antagonists exhibiting IC_{50} values ranging from 1.3 nM to 150 μM. Additionally, a qualitative pharmacophore hypothesis was derived from multiconformational structure models of the two highly active AT_1 antagonists **4u** (IC_{50} = 0.2 nM) and **3k** (IC_{50} = 0.7 nM). In the case of the quantitative model, the best pharmacophore hypothesis consisted of a five-features model (Hypo1: seven points, one hydrophobic aromatic, one hydrophobic aliphatic, a hydrogen bond acceptor, a negative ionizable function, and an aromatic plane function). The best qualitative model consisted of seven features (Hypo2: 11 points, two aromatic rings, two hydrogen bond acceptors, a negative ionizable function, and two hydrophobic functions). The obtained pharmacophore models were validated on a wide set of test molecules. They were shown to be able to identify a range of highly potent AT_1 antagonists, among those a number of recently launched drugs and some candidates presently undergoing clinical tests and/or development phases. The results of our study provide confidence for the utility of the selected chemical feature based pharmacophore models to retrieve structurally diverse compounds with desired biological activity by virtual screening.

Introduction

The renin−angiotensin−aldosteron system (RAAS) has a central role in the expression and modulation of cardiovascular diseases. Renin is the enzyme that cleaves circulating angiotensinogen, a polypeptide produced in the liver, to yield the decapeptide angiotensin I (AI), which is cleaved into the octapeptide angiotensin II (AII) by angiotensin-converting enzyme (ACE). Angiotensinases lead to angiotensin III (AIII), a heptapeptide, and several inactive fragments. ACE inhibitors are widely accepted therapeutics applied in regulation of cardiovascular disorders such as hypertension, congestive heart failure, and vascular disease. An unpleasant limitation of ACE inhibitors is the cleaving of substrates other than angiotensin I, for example, bradykinin. Enzymatic degradation of this peptide vasodilator is reduced by ACE inhibitors. Bradykinin may stimulate nitric oxide (NO) synthesis and the release of prostaglandin I2 and E2 (PGI, PGE). Thus, dry cough, angioedema, aplastic anemia, conjunctivitis, headache paresthesias, and sinus tachycardia are associated side effects of ACE inhibitors.[1] The usage of non-peptide-selective angiotensin II (AII) subtype 1 receptor antagonists represents an approach to intermit cascade at the terminal level. The angiotensin receptor (AT) family is a member among the heptahelical G-protein coupled receptor families and is divided into subtypes AT_1, AT_2, and AT_4. The AT_1 receptor mediates most of the identified vascular effects of angiotensin II.[2] The octapeptide angiotensin II (Asp-Arg-Val-Tyr-Val-His-Pro-Phe) is a potent vasoconstrictor affecting different organ systems, e.g., kidney, blood vessels, smooth muscles, adrenal cortex, medulla, and myocardium. Resulting effects are release of aldosterone, catecholamines, and antidiuretic hormone and lead to increased blood pressure.[3] Since the AT_1 receptor plays a dominant role in intracellular signaling related to blood pressure regulation, we chose this subtype that is coupled to the $G_{q/11}$/phosphoplipase C/inositol 1,4,5-triphosphate/cytosolic calcium channel pathway for our investigations.[4]

Earlier Approaches

In the past years several 3D QSAR (quantitative structure−activity relationship) and modeling studies on angiotensin II and AT_1 receptor antagonists have been performed and reported in the literature.[2,4−7] The results of a homology modeling study point out that one of the most significant interactions of AT_1 antagonists is formed by the acid function interacting with the basic amino acid Lys 199 of the trans membrane unit 5 (TM5) of AT_1 receptors. The ionic interactions may be significant because of their far-reaching effects. Hydrophobic aromatic areas should be important for stabilization of the acid−base interaction by diminishing the dielectric effect of water.[8] Moreover, three common features were presented by 3D QSAR models identifying an electron-rich site and two π-electron-rich sites, corresponding to oxygen or chlorine atoms and the phenyl rings or the sulfonamido oxygen atoms, respectively.[7] The ortho position of the acid functions also seems to be important for twisting the biphenyl groups out of planarity.[6] More information was reported in the literature, describing

* To whom correspondence should be addressed. Phone: +43 512 507 5252. Fax: +43 512 507 5269. E-mail: thierry.langer@uibk.ac.at.
† Phone: +43 512 507 5264. E-mail: eva.krovat@uibk.ac.at.

10.1021/jm021032v CCC: $25.00
Published on Web 02/01/2003

Table 1. Chemical Structures[a] of 25 Training Set Molecules[b] Used To Form HypoGen Pharmacophore Hypotheses

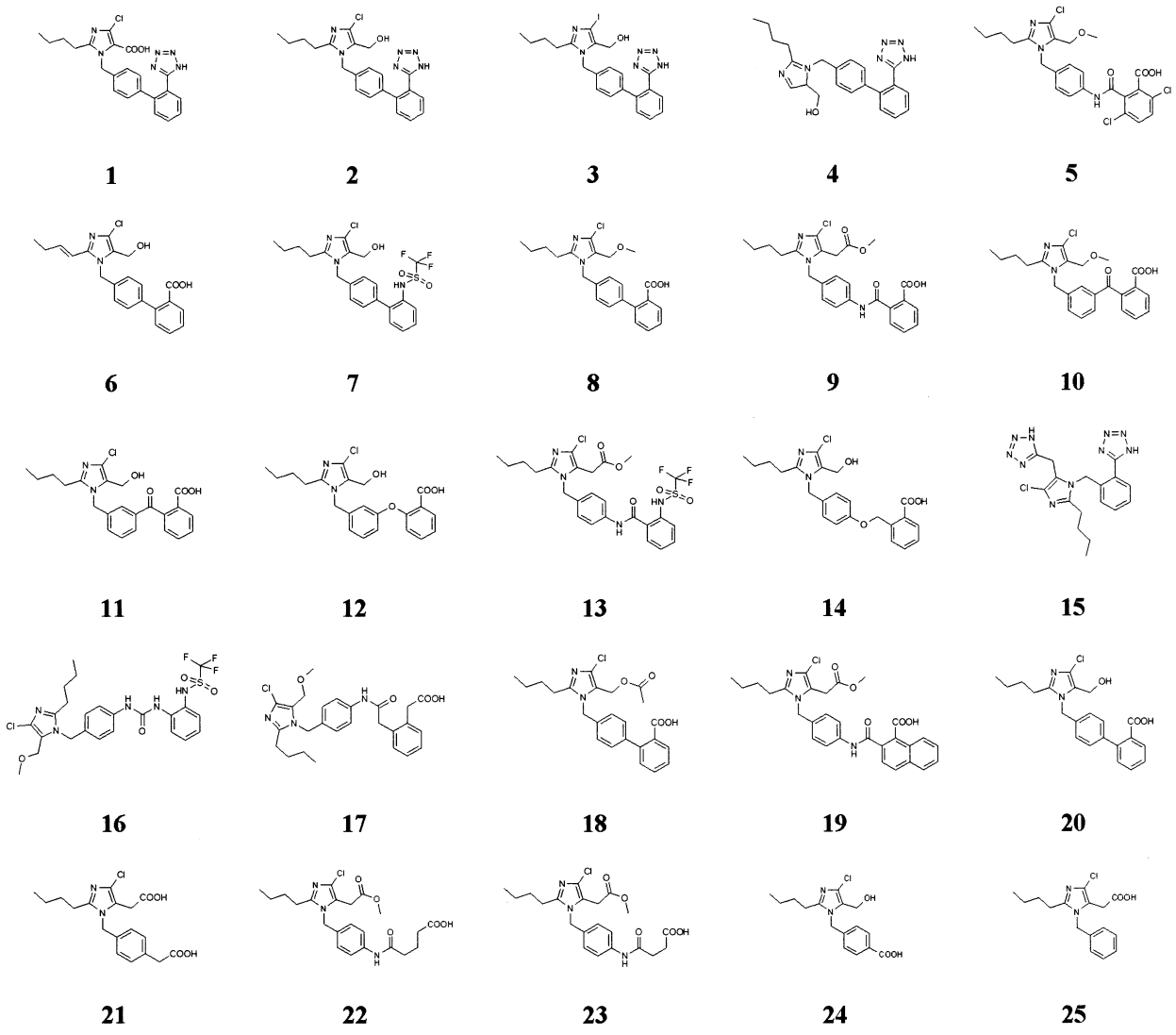

[a] All 2D chemical structures were produced with the *ISIS/Draw*, version 2.1 drawing program.[52] [b] Detailed information of synthesis and biological data is reported elsewhere.[9]

a minimal pharmacophore, including an acidic group, an aromatic N atom functioning as hydrogen bond acceptor, and an alkyl side chain plus a biphenyl spacer.[9] A 3D database search for new bioisostere of BPT (biphenylytetrazole) in order to explore new lead structures yielded molecules featuring subnanomolar K_i values in vitro but unfortunately nearly no biological effect in vivo. Therefore, these new more rigid substructures containing the tricyclic dibenzo[*a*,*d*]cycloheptene or dibenzo[*b*,*f*]oxepine moiety instead of the biphenyl moiety are not a matter of prospective interest.[10]

A powerful approach in virtual drug design is the automated generation of pharmacophore models within the Catalyst software package[11] using two different algorithms (HipHop and HypoGen), as a large number of successful applications in medicinal chemistry clearly demonstrates.[12−30] Debnath has recently reported the development of pharmacophore models from a series of inhibitors of mycobacterium avium complex dihydrofolate reductase (MAC DHFR) and human dihydrofolate reductase (h-DHFR). The model was validated on three structurally diverse classes of compounds that show activity against MAC DHFR.[31] Pharmacophore models are of special interest when experimental data on the biologically relevant conformations of the selected compounds are absent (for example, atomic coordinates derived from X-ray crystallographic studies of protein−ligand complexes are missing, e.g., G-protein coupled receptors).

The aim of this study was to build pharmacophore models based on common chemical features of compounds that exhibit high antagonistic binding quality to the AT_1 receptor site. Using such a model, one should be able to retrieve structures from 3D molecular databases currently in the clinical development phase or even launched or to retrieve structures that can be used as new potentially active candidates.

General Methology

Training Set Selection and Conformational Models. Twenty-five compounds forming the training set[9,32−34] were used to generate HypoGen hypotheses featuring quantitative predictive character. Structures are reported below in Table 1.

The selection of training set members is a key step in automated pharmacophore generation. The constructed pharmacophore model apparently can be as good as the information of data input.[35] Some guidelines for 3D QSAR model generation in Catalyst must be respected. The minimum number of molecules to ensure statistical significance of pharmacophores computed in the HypoGen algorithm is 16; the activity data should span over 4−5 orders of magnitude. The most active compound available must be included, and each order of magnitude should be represented by at least three compounds. Each compound should provide new structural information. The activity data, in this case IC_{50} in μM must be directly comparable i.e., derived from an equivalent analytical method, similar species, and similar tissue. In this study, the activity data were taken from different scientific groups that used equivalent binding assays. A series of angiotensin II subtype 1 receptor antagonists (now termed as AT_1 antagonists) were tested in rat adrenal cortical microsomes preparations for their inhibitory effects on the specific binding of angiotensin II. Binding assays are reported in detail elsewhere.[9,32−34] All structures were built and minimized within the Catalyst software package, and conformational analysis for each molecule was implemented using the Poling algorithm. Poling is a method for promoting conformational variation that forces similar conformers away from each other. Conclusively, poling improves the coverage of the conformational space.[36−38] The settings in conformer generation were 250 as the maximum number of conformers, best quality generation type, and an energy range of 20 kcal/mol beyond the calculated potential energy minimum. All other parameters used were kept at their default settings. This should ensure an exhaustive characterization of conformational space.[11]

Generation of Pharmacophore Hypotheses. A pharmacophore is a representation of generalized molecular features including 3D (hydrophobic groups, charged/ionizable groups, hydrogen bond donors/acceptors), 2D (substructures), and 1D (physical or biological properties) aspects that are considered to be responsible for a desired biological activity. Two different approaches are applied in automated hypothesis generation. The first is HypoGen, an activity-based alignment derived from a collection of conformational models of compounds spanning activities of 4−5 orders of magnitude. Detailed criteria for training set selection are presented earlier. The second algorithm in 3D pharmacophore generation within Catalyst is a common feature-based alignment of highly potent compounds. The activity of several molecules is not regarded using this model generation mode. HipHop hypotheses are produced by comparing a set of conformational models and a number of 3D configurations of chemical features shared among the training set molecules. Compounds of the training set may or may not fit all features of each resulting hypothesis, depending on the setting for the parameters Maximum Omitted Features, Misses, and Complete Misses. The retrieved pharmacophore models are expected to discriminate between active and inactive compounds.

The first step in generation of a pharmacophore model after choosing the training set is the feasible feature selection performed by the user. Each feature is defined by a chemical function, location, and orientation in 3D space, tolerance in location, and weight. Hydrogen bond acceptor (A), hydrophobic (H), hydrophobic aliphatic (Z), hydrophobic aromatic (Y), ring aromatic (R), and negative ionizable (N) were carefully selected for the description of the AT_1 receptor site. Additionally an individually built feature named NegIonizable was edited to identify the weak acid N−H of sulfonamides. This was performed in the Exclude/OR QickTool by extending the default negative ionizable function to include sulfonamides. The modified function was added to the Feature Dictionary to ensure the application in hypothesis generation (Figure 2)

Eq.1 $$MA \times Unc_{MA} - \frac{A}{Unc_A} > 0.0$$

Eq.2 $$\log(A) - \log(MA) > 3.5$$

Eq.3 $$FixedCost = eE(x=0) + wW(x=0) + cC$$

Eq.4 $$NullCost = eE(x=\bar{x})$$

Eq.5 $$Cost = eE + wW + cC$$

Figure 1. Equations describing the HypoGen algorithm. Abbreviations: Unc, uncertainty (default 3); MA, activity of most active compound; *A*, activity of active compound; *E*, error; *e*, error coefficient (default 1); *W*, weight; *w*, weight coefficient (default 1); *C*, configuration; *c*, configuration coefficient (default 1); *x*, deviation from the expected values of weight and error.

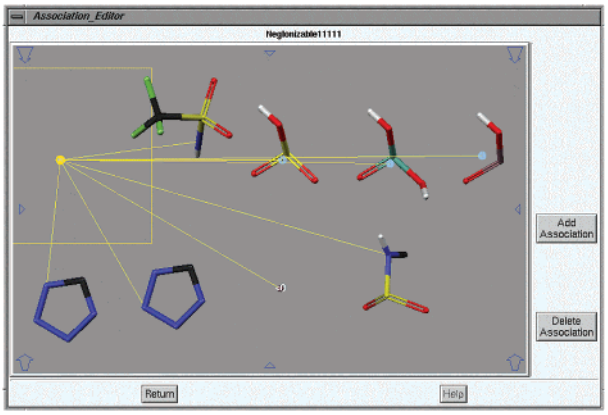

Figure 2. Extended negative ionizable function in the Exclude/OR QickTool including sulfonamides N−H as weak acids.

Database Search. Hypotheses can be used as queries to search 3D databases to retrieve structures that fit the hypothesis or as models to forecast the activities of novel compounds. In this study, a database built in the Catalyst data format containing 138 AT_1 antagonists was used for virtual screening. Additionally a search was pursued within the Derwent World Drug Index (WDI), containing approximately 50 000 drugs worldwide and bioactive molecules with their incidental multiple conformers.[39] A database search in Catalyst involves two algorithms. The Fast Flexible Search Databases/Spreadsheets command computes already existing conformers of the database, the Best Flexible Search Databases/Spreadsheets is able to change the conformation of a molecule during computation. All queries were performed using the Fast Flexible Search Databases/Spreadsheets method. A molecule must fit all the features of a Catalyst query to be retrieved as a hit. Results are hit lists containing those compounds of

the database that fulfill all requirements in 3D space of the hypothesis used as search input.

Results and Discussion

1. HypoGen Model. The biological dataset was divided into a training set, presented in Table 1, and into a test set presented in Table 4. The training set consists of 25 structures and was selected by considering structural diversity and wide coverage of activity range. Activities are reported as IC_{50} values (inhibitory concentration of an inhibitor that gives 50% displacement of the specific binding of labeled angiotensin II) spanning from 1.3 nM to 150 μM. Each compound of the training set should provide new structural information to achieve a good model in terms of predictive power and statistical significance. A default uncertainty factor of 3 for each compound was defined, representing the ratio range of uncertainty in the activity value based on the expected statistical straggling of biological data collection. Uncertainty influences the first of three steps in the HypoGen generating process, as presented in Figure 1, eq 1. The hypothesis created in the initial phase, the constructive phase, considers all possible pharmacophore configurations of the most active compounds to imply pharmacophore demands. In the proximate second phase, the subtractive phase, all possible pharmacophore configurations of the constructive phase are kept or discarded depending on the number of least active training set members that share a pharmacophore pattern. Least active compounds are detected by employing eq 2 in Figure 1. In the final optimization phase, geometric fit, activity, error estimation, and cost calculation are performed. The hypothesis generation process stops when no better score of the hypothesis can be accomplished.[40] Important features for angiotensin II antagonists were described in earlier studies. In the hypothesis generation process, five features (hydrogen bond acceptor (A) and aromatic plane as vector functions (R) and hydrophobic aromatic (Y), hydrophobic aliphatic (Z), and a modified negative ionizable feature (N) as point functions) were selected to form the essential information. The HypoGen algorithm was forced to find pharmacophores that contain at least one and at most two of every feature except the negative ionizable and aromatic plane features. Pharmacophores were computed, and the top 10 hypotheses were exported, consisting of these five features presenting seven-point pharmacophores. (Figure 3). According to earlier submitted pharmacophore studies, the negative ionizable (N), hydrophobic aromatic (Y), hydrophobic aliphatic (Z), ring aromatic (R), and hydrogen bond acceptor (A) features were considered to be important.[32,41,42] Hence, in pharmacophore generation, priorities were set on them. The algorithm was forced to select a certain mininum and maximum number of these features, as explained earlier, regarding the value of configuration cost contribution. Catalyst produced 10 hypotheses: top ranked Outhypo-181690.01, entitled Hypo1 is presented in Figure 3 aligned with the highest active compound (cmp1: 1.3 nM) of the training set molecules. Hypo1 is the best pharmacophore hypothesis in this study, characterized by the highest cost difference, lowest error cost, and lowest root-mean-square divergence and has the best correlation coefficient. All 10 hypotheses contain the same features: one hydrogen bond acceptor, one negative ionizable, one hydrophobic aliphatic, one hydrophobic aromatic, and one ring aromatic feature (Figure 3). The validation of reported hypotheses can be performed in different ways. First, Catalyst applies a cost analysis to reveal statistically significant hypotheses generated with the HypoGen algorithm. Catalyst calculates the cost for a theoretical ideal hypothesis (fixed cost). The choice among many possibilities in spatial arrangements is made according to Occam's razor principle, which states that among equivalent possibilities, the simplest is the best. Three cost values, all of them measured in bits, are crucial in the validation of a pharmacophore model. First, the fixed cost is a theoretical cost value that entirely fulfils all demands of data input (Figure 1, eq 3). Second, the null cost value is the highest of the three values (Figure 1, eq 4). It presents all activities of the training set molecules as average values and represents a hypothesis containing no features. Finally, the total hypothesis cost is the summation of three factors: a weight, an error, and a configuration cost.

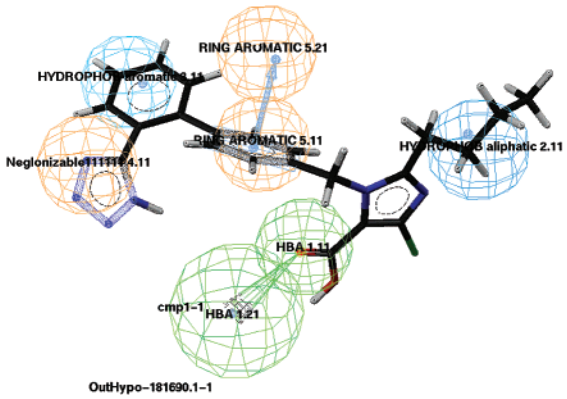

Figure 3. Top scoring HypoGen pharmacophore (five features, seven points). Hypo1 is aligned to the most active compound in the training set (cmp1: IC_{50} = 1.3 nM). Pharmacophore features are color-coded (orange, negative ionizable and aromatic ring; light-blue, hydrophobic aromatic and hydrophobic aliphatic; green, hydrogen bond acceptor).

The mathematical background of total cost calculation is presented in Figure 1, eq 5. Configuration cost is equal to entropy cost, a constant value, and should always be less than 17. The weight component will increase in a Gaussian form as the default value (2.0) deviates. The error cost will increase as will the root-mean-square (rms) factor, which is the divergence of the estimated and actual activity of training set molecules (Table 3). Correlation values are obtained by linear regression of the geometric fit index. Fit functions check mapping of chemical substructure into feature constraints as well as distance deviation of chemical functions from the center of the feature. Therefore, the geometric fit value points out how exact the function is localized in the center of a feature sphere (Figure 1, eq 6).

The correlation coefficient (Table 2) is based on linear regression derived from the geometric fit index. Another validation method to characterize the quality of a hypothesis is represented by its capacity for correct activity prediction. Estimated activity values and errors (ratio between the estimated and tested activity) are reported in Table 3. (For instance, an error of −1.4 means that the experimentally tested activity is 40%

Table 2. Information of Statistical Significance and Predictive Power Presented in Cost Values Measured in Bits for Top 10 Hypotheses as a Result of Automated HypoGen Pharmacophore Generation Process[a]

hypothesis no.	total cost	Δ cost	rms deviation	correlation (r)
1	109.569	63.426	0.739	0.963
2	113.752	59.243	1.004	0.927
3	113.844	59.151	1.026	0.923
4	114.004	58.991	1.045	0.920
5	114.22	58.775	1.067	0.916
6	114.392	58.603	1.028	0.923
7	115.08	57.915	1.089	0.912
8	116.473	56.522	1.133	0.905
9	116.901	56.094	1.156	0.901
10	118.144	54.851	1.201	0.892

[a] Null cost of 10 top-scored hypotheses is 172.995. Fixed cost value is 99.9643. Configuration cost is 14.7493.

Table 3. Experimental Biological Data[a] and Estimated IC_{50} of Training Set Molecules Based on Pharmacophore Model Hypo1[a]

compd	no. in the literature	actual IC_{50} [μM]	estimated IC_{50} [μM]	error	activity scale	estimated activity scale
1	77	0.0013	0.0074	5.7	+++	+++
2	76	0.019	0.014	−1.4	+++	+++
3	106	0.02	0.021	1.1	+++	+++
4	107	0.029	0.015	−2	+++	+++
5	34	0.042	0.2	4.7	+++	++
6	65	0.08	0.1	1.3	+++	++
7	74	0.083	0.095	1.1	+++	+++
8	109	0.099	0.12	1.2	+++	++
9	14	0.14	3.4	24	++	++
10	55	0.15	0.11	−1.4	++	++
11	54	0.34	1.9	5.5	++	++
12	56	0.4	0.04	−10	++	+++
13	40	0.5	4.6	9.1	++	++
14	58	0.92	1.2	1.3	++	++
15	39	1.2	10	8.4	++	+
16	62	2.4	10	4.2	++	+
17	23	2.8	7.1	2.5	++	++
18	118	3.33	0.12	−28	++	++
19	16	5.8	3	−2	++	++
20	83	11	10	−1.1	+	+
21	20	13	10	−1.3	+	+
22	12	32	10	−3.2	+	+
23	11	46	10	−4.6	+	+
24	19	100	10	−10	+	+
25	3	150	10	−15	+	+

[a] Activity scale: highly active (<0.1 μM, +++), moderately active (0.1−10 μM, ++), and inactive (>10 μM, +). Detailed information of synthesis and biological data is reported elsewhere.[9]

lower than the predicted, referring to the pharmacophore model.)

Hypotheses are believed to be statistically relevant when the overall hypothesis cost is close to the fixed and far away from null cost values. The difference between the null cost hypothesis and the total hypothesis cost is of particular importance. A true correlation will be estimated very likely by models that exhibit a cost difference (Δ cost = null cost − total cost) of 60 bits or higher. The difference between fixed and null costs should be 70 or higher to achieve this request. Cost differences of 40−60 bits lead to a predictive correlation probability of 75−90%. When cost differences fall under 40, the chance of a true correlation coefficient will probably decrease to 50%. These output parameters determine the quality of pharmacophore hypotheses.[35,43,44] The null cost of the 10 top-scored hypotheses is 172.995, and the fixed cost value is 99.9643. Configuration cost is 14.7493 (Table 2).

Third, another approach to assess the statistical confidence of HypoGen models is to apply cross validation using the CatScramble program. This random test validation helps to define the SAR (structure−activity relationship) of training set members. CatScramble mixes up activity values of all training set compounds and creates in our case 49 random spreadsheets (essential to achieve a statistical significance level of 98%). A HypoGen computation with each of them is performed by keeping the parameters of the initial run of Hypo1. In our case, a statistical significance of 98% was allocated.

All compounds of this study were classified by their activity as highly active (<0.1 μM, +++), moderately active (0.1−10 μM, ++), or inactive (>10 μM, +). All inactive compounds were predicted correctly, two moderately active compounds were predicted to be inactive, and one moderately active compound was predicted to be highly active. All but three of the highly actives were predicted correctly. Altogether, for 19 of 25 compounds, the predicted IC_{50} values were found to be within the same order of magnitude as the experimentally determined ones.

Finally, to check the predictive power of this pharmacophore hypothesis, a test set containing 25 AT_1 antagonists of different activity classes was analyzed. All test set molecules were built and minimized as well as used in conformational analysis like all training set compounds. Hypo1 was regressed against the training set compounds. A score of 85.28% was achieved.

Structural data of test set compounds are shown in Table 4. In the test set analysis, out of six highly active compounds, three were predicted correctly but three highly actives were underestimated as moderately active. All other members of the test set were predicted correctly or as better than their actual activities. Five inactive compounds were regarded as moderately active and therefore are false positives. The results are presented in Table 5.

The mapping of Hypo1 onto a highly active compound of the test set, compound **2** (IC_{50} = 12 nM), is shown in Figure 4. Test set compound **2** fits very well all features of the pharmacophore model Hypo1. The biphenylyltetrazole moiety seems to be essential for high binding affinity, but also compounds containing different structures map all features of Hypo1, e.g., test set compound **2** or **7** shows high affinity.

Quite often, the negative ionizable feature is fitted by tetrazole rings, carboxylic acids, or sulfonamides. In this case, the negative ionizable sphere is mapped by a sulfonic acid. The two hydrophobic aromatic features are fitted by two phenyl rings. In most AT_1 antagonists, the biphenylyl substructure is included, which indicates this moiety to be indispensable for angiotensin II binding affinity.

The pharmacophore model Hypo1 was used in a 3D database query to find new structures mapping this hypothesis. Hypo1 was able to detect 176 of the entire WDI (48 405) substances (~0.4%). To be exported as a hit, they must map the hypothesis in all five features. All compounds exhibiting fit values higher than 5 are reported as AT_1 antagonists in the WDI. The database search procedure, however, also retrieved compounds with activity keywords or mode of action different from

Table 4. Chemical Structures[a] of 25 Diverse Molecules Forming the Test Set

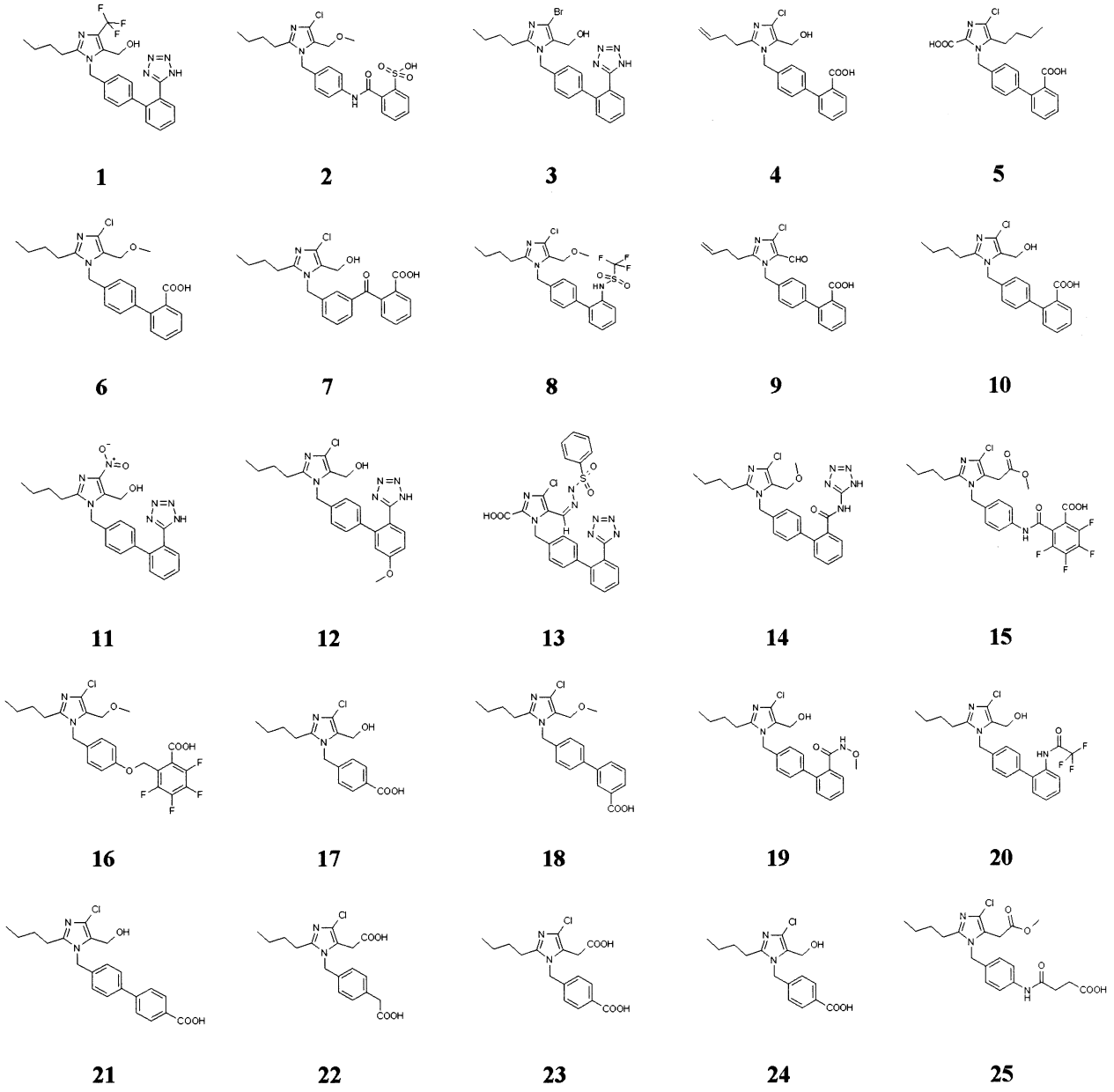

[a] All 2D chemical structures were produced with the *ISIS/Draw*, version 2.1, drawing program.[52]

angiotensin II antagonism. For example, CL-329167 was retrieved, which is reported to act as a somatoliberine agonist (fit value of 5.06), and the leuktotriene antagonist LY-223982[45] (fit value of 4.38) was found.

Another interesting molecule is the viruzide cibatron (fit value of 3.93). A problem related to this hypothesis is obviously the selectivity in filtering WDI compounds, which may be considered as being too high. Some important compounds may not be discovered because of the extensive spatial demands of a five-feature pharmacophore hypothesis. This objection was confirmed by using a subset of the WDI, restricted to 66 non-peptide substances with known angiotensin antagonistic activity, in another 3D database search. Only 25 compounds (37% of the total set) were found. When Hypo1 is modified, for example, when the constraint restrictions are eased or the negative ionizable and aromatic sphere are removed manually, 42 of 66 (63%) can be detected.

The metadata information within the WDI (mechanism of action, activity keywords, indications, usage, ...) is only a subtle hint and is not a significant validation method. Some of the compounds will not be retrieved because the conformers of the WDI do not allow mapping of all features, or some of the compounds in the subset do not fit the negative ionizable function because they act as prodrugs, such as esters. Examples of the WDI subset structures are shown in Figure 5.

In the 3D database containing 138 AT_1 antagonists built within Catalyst, Hypo1 was able to retrieve 129 molecules (93.5%). Three examples of chemical structures included in this data set are shown in Figure 6. Included compounds are AT_1 antagonists that have been recently launched or are in a clinical development stage. Results of this query can be interpreted as a good validation for the generated pharmacophore hypothesis because 93.5% of active AT_1 antagonists were identified as potential candidates. Actual and estimated activity

Table 5. Experimental Biological Data[a] and Estimated IC_{50} of Test Set Molecules Based on Pharmacophore Model Hypo1[a]

test set	no. in the literature	actual IC_{50} [μM]	estimated IC_{50} [μM]	error	actual activity scale	estimated activity scale
1	108	0.012	0.06	5	+++	+++
2	45	0.012	0.39	33	+++	++
3	105	0.019	0.054	2.9	+++	+++
4	65	0.08	0.11	1.3	+++	++
5	64	0.092	0.075	−1.2	+++	+++
6	48	0.099	0.19	1.9	+++	++
7	53	0.16	0.18	1.1	++	++
8	75	0.19	0.1	−1.8	++	++
9	66	0.22	0.04	−5.5	++	+++
10	46	0.23	0.14	−1.6	++	++
11	103	0.26	0.058	−4.5	++	+++
12	88	0.51	0.079	−6.4	++	+++
13	122	0.6	0.22	−2.7	++	++
14	79	0.7	0.91	1.3	++	++
15	27	0.79	2	2.5	++	++
16	60	1.2	2.8	2.4	++	++
17	18	1.7	0.14	−1.6	++	++
18	52	2.9	1.1	−2.7	++	++
19	68	4.1	9	2.2	++	++
20	73	6.3	9	1.4	++	++
21	51	11	9	−1.2	+	++
22	20	13	9	−1.4	+	++
23	19	19	9	−2.1	+	++
24	22	28	9	−3.1	+	++
25	12	32	9	−3.5	+	++

[a] Activity scale: highly active (<0.1 μM, +++), moderately active (0.1−10 μM, ++), and inactive (>10 μM, +). Detailed information of synthesis and biological data is reported elsewhere.[9]

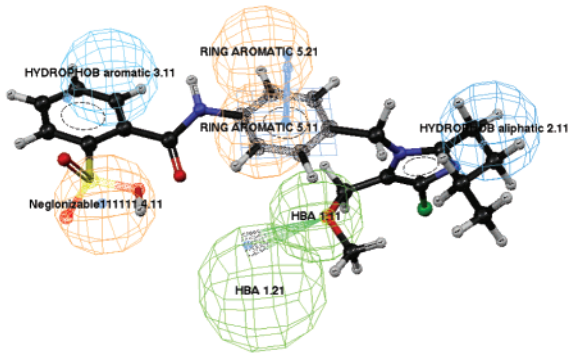

Figure 4. Best HypoGen pharmacophore model Hypo1 aligned to test set cmp2 (IC_{50} = 12 nM). Pharmacophore features are color-coded (orange, negative ionizable and aromatic ring; light-blue, hydrophobic aromatic and hydrophobic aliphatic; green, hydrogen bond acceptor).

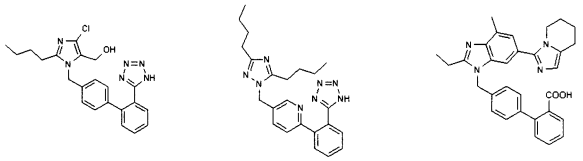

Losartan **Forasartan** **Pomisartan**

Figure 5. Three examples of chemical structures included in the WDI subset database of 66 AT_1 antagonists.

data were not scored because of different assay systems used by different research groups. In Figure 7, four structurally diverse compounds antagonizing the angiotensin II subtype 1 (AT_1) receptor are presented as an example. The information of pharmacophore Hypo1 may be useful in the development of new drugs inhibiting the angiotensin II subtype 1 (AT_1) receptor.

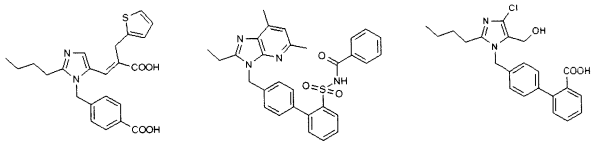

Eprosartan **MK966** **EXP7711**

Figure 6. Three examples of chemical structures included in the 138 compounds Catalyst database.

2. HipHop Model. The algorithm for qualitative pharmacophore model generation applied within Catalyst is termed HipHop. This method is used when the ligand set is small and sufficient biological data are not available. In this case, the alignment of some highly potent compounds can lead to a spatial arrangement of common chemical features of the molecules forming the training set. Each member of the training set is represented by a collection of conformers that should be able to extensively cover the conformational space 20 kcal/mol beyond the calculated potential energy minimum. After the conformation models are generated, all conformers are aligned, regarding the chemical feature demanded by the user. Finally a 3D configuration of common chemical features of training set molecules is determined.[46]

In our case, two highly potent AT_1 antagonists (**4u**, IC_{50} = 0.2 nM; **3k**, IC_{50} = 0.7 nM) were selected to form the basis information of this computational method.[41] Hypo2 (Outhypo 55649.01, Figure 8) compiles the feature requirements of the training set considered as relevant. In the hypothesis generation, Catalyst was forced to find a model including two ring aromatic (R) features, one hydrophobic (H), two hydrogen bond acceptors (A), and one negative ionizable (N) function (Figure 6). Both molecules were set as principals, which means that all features must be mapped. The output hypothesis is composed of seven features and 11 spheres: two aromatic rings, two hydrophobic groups (one more than expected), two hydrogen bond acceptors, and one negative ionizable function. Hypo2 was used as a query in a 3D database.[41] An amount of 42 out of 46 substances featuring IC_{50} values of 20 nM or better were retrieved. This would indicate that this model is able to retrieve 91% of the highly active compounds. Additionally 14 out of 36 less active AT_1 antagonists (20−500 nM) were found. According to our expectations, this pharmacophore model was able to identify a number of recently launched AT_1 antagonists or some that are presently undergoing the clinical test/development phase. (Table 6).

In the Catalyst AT_1-antagonist-subset database, 98 of 138 AT_1 antagonists mapped the hypothesis as direct hits. New compounds reported recently in the literature were found in the query.[6,41,47−50] The 3D database search in WDI resulted in only 73 structures (0.15% of the entire WDI). Thirty-seven of them were registered in the ensemble database[45] as AT_1 antagonists, six as AT_1/AT_2 antagonists, and one as ACE inhibitor. Thirty compounds of the hit list were not found in the ensemble database. All hits of the WDI search containing 1D information indicate their mode of action as AT_1 antagonists. In the subset of 66 non-peptide AT_1 antagonists, only 17 are detected because of earlier described

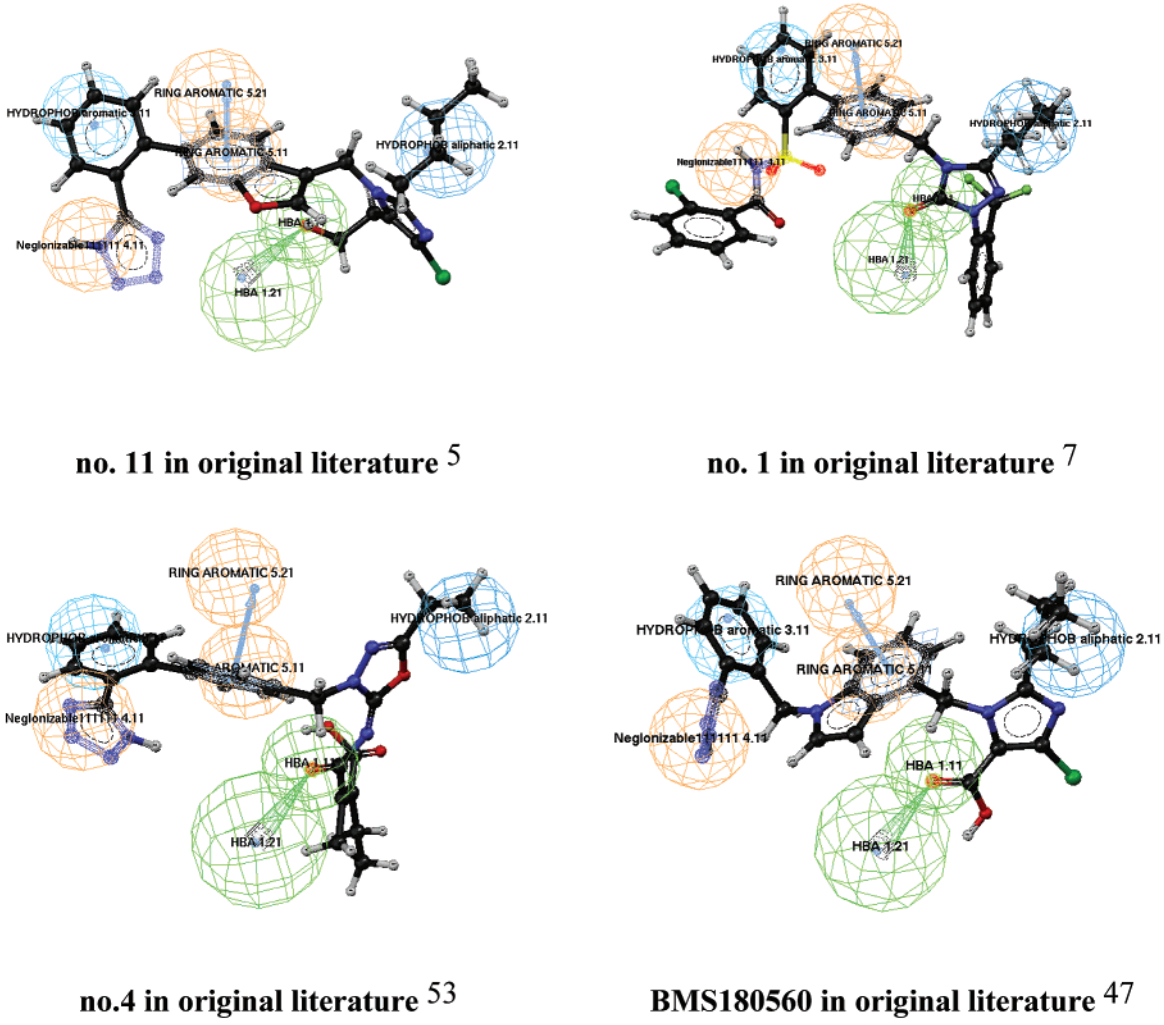

Figure 7. Four examples of compounds antagonizing the angiotensin II subtype 1 receptor. Pharmacophore features are color-coded (orange, negative ionizable and aromatic ring; light-blue, hydrophobic aromatic and hydrophobic aliphatic; green, hydrogen bond acceptor).

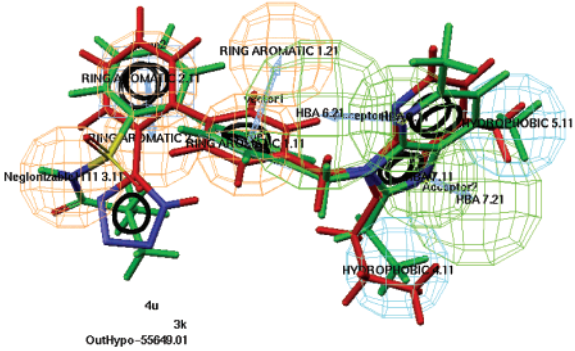

Figure 8. Hypo2 and two training set compounds. **3k** shows $IC_{50} = 0.7$ nM and **4u** shows $IC_{50} = 0.2$ nM. Pharmacophore features are color-coded (orange, negative ionizable and aromatic ring; cyan, hydrophobic; green, hydrogen bond acceptor).

causes. Molecules mapped on Hypo2 containing diverse substructures to BPT (biphenylytetrazole) are presented in Figure 9.

Conclusions and Perspectives

The pharmacophore models generated in this study highlight the pattern with significance for antagonistic activity on the AT_1 receptor site. In this work, two different approaches were performed to describe the essential pharmacophore of the AT_1 receptor antagonists. With both the HypoGen and the HipHop algorithms within the Catalyst software, several models

Table 6. Compounds Sorted by Descending Geometric Fit Values[a]

compd	generic name or company code	current development phase
1	milfasartan	phase 2
2	Cl-329167	phase 2
3	EXP-3174	phase 3
4	ripisartan	phase 2
5	irbesartan	launched 97
6	candesartan	phase 1
7	YM-358	phase 2
8	forasartan	phase 2
9	zolasartan	phase 2
10	losartan	launched 94
11	pomisartan	phase 2
12	L-159282	phase 2
13	saprisartan	phase 2
14	fonsartan	phase 2
15	tasosartan	preregistered
16	valsartan	launched 96

[a] According to our expectations, pharmacophore model Hypo2 was able identify a number of recently launched AT_1 antagonists or some presently undergoing clinical test/development phase. Generic name or company codes and development phase are retrieved from a purchasable database.[45]

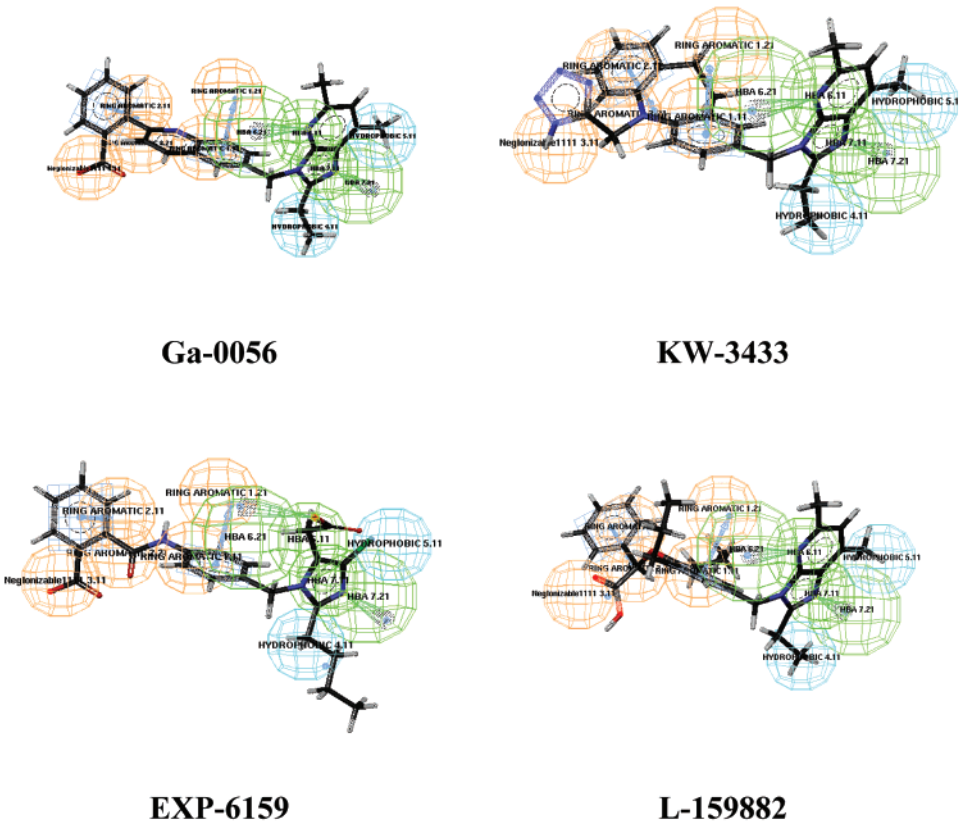

Figure 9. Mapping of four molecules containing diverse substructures to biphenlylytetrazole (BPT) used as proof of the predictive power of the model. Pharmacophore features are color-coded (orange, negative ionizable and aromatic ring; cyan, hydrophobic; green, hydrogen bond acceptor).

were obtained. The best pharmacophore in terms of predictive value consisted of a five-feature HypoGen model (Hypo1, seven points with one hydrophobic aromatic, one hydrophobic aliphatic, a hydrogen bond acceptor, a negative ionizable function, and an aromatic plane function) and of a seven-feature HipHop model (Hypo2, 11 points with two aromatic rings, two hydrogen bond acceptors, a negative ionizable function, and two hydrophobic functions). The pharmacophores were able to identify a range of highly potent AT_1 antagonists. All compounds of the training set were mapped in both approaches as direct hits. Also, AT_1 antagonists outside the training set fitted onto most of the features considered important for activity. When the pharmacophore model generated with HypoGen (Hypo1) is compared to the ones built with HipHop (Hypo2), Hypo1 finds more AT_1 antagonists. The hydrophobic aromatic functions in Hypo1 are one-point features and hence represent a less specific filter than the two-point vector function of the aromatic plane in Hypo2. Most active compounds will fit some of these recommended chemical features but maybe not all of them. All those molecules are ignored in the database search because only thorough-fitting compounds are reported as hits. Eased-constraint tolerances could be useful to eventually reveal more active compounds. At the same time, the probability of finding false positives increases. A false positive in a hit list does not necessarily mean that the compound is inactive. Molecules without the expected 1D information can also show affinity and therefore be interesting leads. The generation of a subset database can help to evaluate models, but success is limited to quality of data content. The aim of pharmacophores can be seen in a 3D database search to find diverse structures with potential activity. The knowledge of important chemical features for AT_1 antagonism is expected to be useful in the development of AT_1 antagonists, e.g., to estimate the activity potential of new designed compounds in virtual libraries, before further investigations are implemented. The utility of our pharmacophores is shown by the fact that the models elaborated within this study were able identify a number of recently launched AT_1 antagonists and some compounds presently undergoing the clinical test and/or development phase. We intend to use our models to discover novel potential AT_1 antagonists within virtual combinatorial databases as generated with our recently developed tool Comb^{i}Gen.[51]

Experimental Section

All molecular modeling studies were performed using Catalyst 4.7 installed on a Silicon Graphic O_2 desktop workstation equipped with a 200 MHz MIPS R5000 processor (128 MB RAM) running the Irix 6.5 operating system. All 2D chemical structures were produced within ISIS/Draw2.1 drawing program.[52]

Acknowledgment. We thank Dr. Rémy D. Hoffmann (Accelrys Inc., Paris) for helpful discussions and for performing the search in the Derwent World Drug Index, as well as Konstantin Poptodorov (University of Innsbruck, presently with Accelrys Inc., Cambridge) for his dedicated support.

Supporting Information Available: All control parameter settings and results of the pharmacophore generation processes plus three-dimensional coordinates of all selected pharmacophore hypotheses (log files generated by the Hypo-

Gen and HipHop algorithms). This material is available free of charge via the Internet at http://pubs.acs.org.

References

(1) Sandow, N. Angiotensin Converting Enzyme (ACE) Inhibitors: Side Effects and Adverse Reactions. http://www.rxlist.com/aceinh.htm (accessed 2002).

(2) Tabibiazar, R.; Jamali, A. H.; Rockson, S. G. Formulating Clinical Strategies for Angiotensin Antagonism: A Review of Preclinical and Clinical Studies. *Am. J.Med.* **2001**, *110*, 471−480.

(3) Pitt, B.; Konstam, M. A. Overview of Angiotensin II−Receptor Antagonists. *Am. J. Cardiol.* **1998**, *82*, 47−49.

(4) Boucard, A. A.; Wilkes, B. C.; Laporte, S. A.; Escher, E.; Guillemette, G.; Leduc, R. Photolabeling Identifies Position 172 of the Human AT1 Receptor as a Ligand Contact Point: Receptor-Bound Angiotensin II Adopts an Extended Structure. *Biochemistry* **2000**, *39*, 9662−9670.

(5) Yoo, S.; Kim, S.; Lee, S.; Kim, N.; Lee, D. The Conformation and Activity Relationship of Benzofuran Type of Angiotensin II Receptor Antagonists. *Bioorg. Med. Chem.* **2000**, *8*, 2311−2316.

(6) Kurup, A.; Gary, R.; Carini, D. J.; Hansch, C. Comparative QSAR: Angiotensin II Antagonists. *Chem. Rev.* **2001**, *101*, 2727−2750.

(7) Pandya, T.; Pandey, S. K.; Tiwari, M.; Chaturvedi, S. C.; Saxena, A. K. 3-D-QSAR Studies of Triazolinone Based Balanced AT1/AT2 Receptor Antagonists. *Bioorg. Med. Chem.* **2001**, *9*, 291−300.

(8) Underwood, D. J.; Strader, C. D.; Rivero, R.; Patchett, A. A.; Grenlee, W.; Prendergast, K. Structural model of antagonist and agonist binding to the angiotensin II, AT1 subtype, G protein coupled receptor. *Chem. Biol.* **1994**, *1*, 211−221.

(9) Duncia, J. V.; Carini, D. J.; Chiu, A. T.; Johnson, A. L.; Price, W. A.; Wong, P. C.; Wexler, R. R.; Timmermans, P. B. M. W. The Discovery of DuP 753, a Potent, Orally Active Nonpeptide Angiotenisin II Receptor Antagonist. *Med. Res. Rev.* **1992**, *12*, 149−191.

(10) Kiyama, R.; Honma, T.; Hayashi, K.; Ogawa, M.; Hara, M.; Fujimoto, M.; Fujishita, T. Novel Angiotensin II Receptor Antagonists. Design, Synthesis, and in Vitro Evaluation of Dibenzo[*a*,*d*]cycloheptene and Dibenzo[*b*,*f*]oxepin Derivates. Searching for Bioisosteres of Biphenyltetrazole Using a Three-Dimensional Search Technique. *J. Med. Chem.* **1995**, *28*, 2728−2741.

(11) *Catalyst*, version 4.7 (software package); Accelrys, Inc. (previously known as Molecular Simulations, Inc.): San Diego, 2002.

(12) Saladino, R.; Crestini, C.; Palamara, A. T.; Danti, M. C.; Manetti, F.; Corelli, F.; Garaci, E.; Botta, M. Synthesis, Biological Evaluation, and Pharmacophore Generation of Uracil, 4(3*H*)-Pyrimidone, and Uridine Derivates as Potent and Selective Inhibitors of Parainfluenza 1 (Sendai) Virus. *J. Med. Chem.* **2001**, *44*, 4554−4562.

(13) Tafi, A.; Costi, R.; Botta, M.; Di Santo, R.; Corelli, F.; Massa, S.; Ciacci, A.; Manetti, F.; Artico, M. Antifungal Agents. 10. New Derivates of 1-[(Arly)[4-aryl-1*H*-pyrrol-3-yl]methyl]-1*H*-imidazole, Synthesis, Anti-Candida Activity, and Quantitative Structure−Analysis Relationship Studies. *J. Med. Chem.* **2002**, *45*, 2720−2732.

(14) Singh, J.; van Vlijmen, H.; Liao, Y.; Lee, W.; Cornebise, M.; Harris, M.; Shu, I.; Gill, A.; Cuervo, J. H.; Abraham, W. M.; Adams, S. P. Identification of Potent and Novel $\alpha 4\beta 1$ Antagonists Using in Silico Screening. *J. Med. Chem.* **2002**, *45*, 2988−2993.

(15) Palomer, A.; Cabre, F.; Pascual, J.; Campos, J.; Trujillo, M. A.; Entrena, A.; Gallo, M. A.; Garcia, L.; Mauleon, D.; Espinosa, A. Identification of Novel Cyclooxygenase-2 Selective Inhibitors Using Pharmacophore Models. *J. Med. Chem.* **2002**, *45*, 1402−1411.

(16) Ekins, S.; Kim, R. B.; Leake, B. F.; Dantzig, A. H.; Schuetz, E. G.; Lan, L.; Yasuda, K.; Shepard, R. L.; Winter, M. A.; Schuetz, J. D.; Wikel, J. H.; Wrighton, S. A. Application of Three-Dimensional Quantitative Structure−Activity Relationships of P-Glycoprotein Inhibitors and Substrates. *Mol. Pharmacol.* **2002**, *61*, 974−981.

(17) Dziadulewicz, E. K.; Ritchie, T. J.; Hallett, A.; Snell, C. R.; Davies, J. W.; Wrigglesworth, R.; Dunstan, A. R.; Bloomfield, G. C.; Drake, G. S.; McIntyre, P.; Brown, M. C.; Burgess, G. M.; Lee, W.; Davis, L.; Yaqoob, M.; Phagoo, S. B.; Phillips, E.; Perkins, M. N.; Campbell, E. A.; Davis, A. J.; Rang, H. P. Nonpeptide Bradykinin B_2 Receptor Antagonists: Conversion of Rodent-Selective Bradyzide Analogues into Potent, Orally Active Human Bradykinin B_2 Receptor Antagonists. *J. Med. Chem.* **2001**, *45*, 2160−2172.

(18) Flohr, S.; Kurz, M.; Kostenis, E.; Brkovich, A.; Fourier, A.; Klabunde, T. Identification of Nonpeptidic Urotensin II Receptor Antagonists by Virtual Screening Based on a Pharmacophore Model Derived from Structure−Activity Relationships and Nuclear Resonance Studies on Urotensin II. *J. Med. Chem.* **2002**, *45*, 1799−1805.

(19) Kurogi, Y.; Miyata, K.; Okamura, T.; Hashimoto, K.; Tsutsumi, K.; Nasu, M.; Moriyasu, M. Discovery of Novel Mesangial Cell Proliferation Inhibitors Using a Three-Dimensional Database Searching Method. *J. Med. Chem.* **2001**, *44*, 2304−2307.

(20) Chen, G. S.; Chang, C.; Kan, W. M.; Chang, C.; Wang, K. C.; Chern, J. Novel Lead Generation through Hypothetical Pharmacophore Three-Dimensional Database Searching: Discovery of Isoflavonoids as Nonsteroidal inhibitors of Rat 5α-Reductase. *J. Med. Chem.* **2001**, *44*, 3759−6763.

(21) Palomer, A.; Pascual, J.; Cabré, F.; Luisa, M.; Mauleón, D. Derivation of Pharmacophore and CoMFA Models for Leukotriene D_4 Receptor Antagonists of the Quinolinyl(bridged)aryl Series. *J. Med. Chem.* **2000**, *43*, 392−400.

(22) Kaminski, J. J.; Rane, D. F.; Snow, M. E.; Weber, L.; Rothofsky, M. L.; Anderson, S. D.; Lin, S. L. Identification of Novel Farnesyl Protein Transferase Inhibitors Using Three-Dimensional Database Searching Methods. *J. Med. Chem.* **1997**, *40*, 4103−4112.

(23) Barbaro, R.; Betti, L.; Botta, M.; Corelli, F.; Giannacchini, G.; Maccari, L.; Manetti, F.; Strappaghetti, G.; Corsano, S. Synthesis, Biological Evaluation, and Pharmacophore Generation of New Pyridazinone Derivates with Affinity toward α_1- and α_2-Adrenoceptores. *J. Med. Chem.* **2001**, *44*, 2118−2132.

(24) Ekins, S.; Durst, G. L.; Stratford, R. E.; Thorner, D. A.; Lewis, R.; Lonarich, R. J.; Wikel, J. H. Three-Dimensional Quantitative Structure−Permeability Relationship Analysis for a Series of Inhibitors of Rhinovirus Replication. *J. Chem. Inf. Comput. Sci.* **2001**, *41*, 1578−1586.

(25) Bureau, R.; Daveu, C.; Lemaître, S.; Dauphin, F.; Landelle, H.; Lancelot, J.; Rault, S. Molecular Design Based on 3D-Pharmacophore. Application to 5-HT_4 Receptor. *J. Chem. Inf. Comput. Sci.* **2002**, *42*, 962−967.

(26) Bureau, R.; Daveu, C.; Lancelot, J.; Rault, S. Molecular Design Based on 3D-Pharmacophore. Application to 5-HT Subtypes Receptors. *J. Chem. Inf. Comput. Sci.* **2002**, *42*, 429−436.

(27) Greenidge, P. A.; Weiser, J. A comparison of methods for pharmacophore generation with the catalyst software and their use for 3D-QSAR: application to a set of 4-aminopyridine thrombin inhibitors. *Mini-Rev. Med. Chem.* **2001**, *1*, 79−87.

(28) Baringhaus, K. H.; Matter, H.; Stengelin, S.; Kramer, W. Substrate specificity of the ileal and the hepatic Na^+/bile acid cotransporters of the rabbit. II. A reliable 3D QSAR pharmacophore model for the ileal Na^+/bile acid cotransporter. *J. Lipid Res.* **1999**, *40*, 2158−2168.

(29) Manetti, F.; Corelli, F.; Biava, M.; Fioavanti, R.; Porretta, G. C.; Botta, M. Building a pharmacophore model for a novel class of antitubercular compounds. *Farmaco* **2000**, *55*, 484−491.

(30) Ekins, S.; Crumb, W. J.; Dustan, S.; Wikel, J. H.; Wrighton, S. A. Three-Dimensional Quantitative Structure−Activity Relationship for Inhibition of Human Ether-a-Go-Go-related Gene Potassium Channel. *J. Pharmacol. Exp. Ther.* **2002**, *301*, 427−434.

(31) Debnath, A. K. Pharmacophore Mapping of a Series of 2,4-Diamino-5-Reductase. *J. Med. Chem.* **2002**, *45*, 41−53.

(32) Duncia, J. V.; Chiu, A. T.; Carini, D. J.; Gregory, G. B.; Johnson, A. J.; Price, W. A.; Wells, G. J.; Wong, P. C. C.; Timmermans, P. B. W. M.; The Discovery of Potent Nonpeptide Angiotensin II Receptor Antagonists: A New Class of Potent Antihypertensives. *J. Med. Chem.* **1990**, *33*, 1312−1329.

(33) Carini, D. J.; Duncia, J. V.; Johnson, A. L.; Chiu, A. T.; Price, W. A.; Wong, P. C.; Timmermans, P. B. M. W. Nonpeptide Angiotensin II Receptor Antagonists: *N*-[(Benzyloxy)benzyl]-imidazoles and Related Compounds as Potent Antihypertensives. *J. Med. Chem.* **1990**, *33*, 1330−1336.

(34) Wong, P. C.; Price, W. A., Jr.; Chiu, A. T.; Carini, D. J.; Duncia, J. V.; Johnson, A. L.; Wexler, R. R.; Timmermans, P. B. M. W. Nonpeptide Angiotensin II Receptor Antagonists. Studies with EXP9270 and DuP 735. *Hypertension* **1990**, *15*, 823−834.

(35) Sutter, J.; Güner, O.; Hoddmann, R.; Li, H.; Waldman, M. In *Pharmacophore, Perception, Development and Use in Drug Design*; Güner, O. F., Ed.; International University Line: La Jolla, CA, 2000; pp 504−506.

(36) Smellie, A.; Kahn, S. D.; Teig, S. L. Analysis of Conformational Coverage. 1. Validation and Estimation of Coverage. *J. Chem. Inf. Comput. Sci.* **1995**, *35*, 285−294.

(37) Smellie, A.; Kahn, S. D.; Teig, S. L. Analysis of Conformational Space. 2. Applications of Conformational Models. *J. Chem. Inf. Comput. Sci.* **1995**, *35*, 295−304.

(38) Smellie, A. Poling: Promoting Conformational Variation. *J. Comput. Chem.* **1995**, *16*, 171−187.

(39) World Drug Index is available in the Catalyst software package, version 4.

(40) Kurogi, Y.; Güner, O. F. Pharmacophore Modeling and Three-Dimensional Database Searching for Drug Design Using Catalyst. *Curr. Med. Chem.* **2001**, *8*, 1035−1055.
(41) Prendergast, K. A., K.; Greenlee, W. J.; Nachbar, R. B.; Patchett, A. A.; Underwood, D. J. Derivation of a 3D pharmacophore model for the angiotensin-II site one receptor. *J. Comput.-Aided Mol. Des.* **1994**, *8*, 491−512.
(42) Ellingboe, J. W.; Collini, M. D.; Quagliato, D.; Chen, J.; Antane, M.; Schmid, J.; Hartupee, D.; White, V.; Park, C. H.; Bagli, J. F.; Tanikella, T. Metabolites of the Angiotensin II Antagonist Tasosartan: The Importance of a Second Acidic Group. *J. Med. Chem.* **1998**, *41*, 4251−4260.
(43) Accelrys, I. Cost analysis in HypoGen. http://www.accelrys.com/doc/life/catalyst47/help/HypoGenAlgRef.doc.html (accessed 2002).
(44) Li, H.; Sutter, J.; Hoffmann, R. HypoGen: An Automated System for Generating 3D Predictive Pharmacophore Models. In *Pharmacophore Perception, Development, and Use in Drug Design*; International University Line: La Jolla, 2000; pp 174−189.
(45) Ensemble. Prous Science Ensemble: A new database affording a unique, integrated view of drug information. http://www.prous.com (accessed 2000).
(46) Li, H.; Sutter, J.; Hoffmann, R. HipHop: Pharmacophores Based on Multiple Common-Feature Alignments. In *Pharmacophore Perception, Development, and Use in Drug Design*; International University Line: La Jolla, 2000; pp 71−84.
(47) Wexler, R. R.; Greenlee, W. J.; Irvin, J. D.; Goldberg, M. R.; Prendergast, K.; Smith, R. D.; Timmermans, P. B. M. W. M. Nonpeptide Angiotensin II Receptor Antagonists: The Next-Generation in Antihypertensive Therapy. *J. Med. Chem.* **1996**, *39*, 625−656.
(48) Zanka, A.; Nishiwaki, M.; Morinaga, Y.; Inoue, T. Pilot Scale Synthesis of a Novel Nonpeptide Angiotensin II Receptor Antagonists. *Org. Process Res. Dev.* **1998**, *1998*, 230−237.
(49) Salimbeni, A.; Canevotti, R.; Paleari, F.; Poma, D.; Caliari, S.; Fici, F.; Cirillo, R.; Renzetti, A. R.; Subissi, A.; Belvisi, L.; Bravi, G.; Scolastico, C.; Giachetti, A. N-3-Substituted Pyrimidones as Potent, Orally Active, AT1 Selective Angiotensin II Receptor Antagonists. *J. Med. Chem.* **1995**, *38*, 4806−4820.
(50) Le Bourdonnec, B.; Meulon, E.; Yous, S.; Goossens, J.-F.; Houssin, R.; J.-P.H. Synthesis and Pharmacological Evaluation of New Pyrazolidine-3,5-dione as AT1 Angiotensin II Receptor Antagonists. *J. Med. Chem.* **2000**, *43*, 2685−2697.
(51) Wolber, G.; Langer, T. In *Rational Approaches to Drug Design*; Höltje, H.-D., Sippl, W., Eds.; Prous Science: Barcelona, 2001, p 390−399.
(52) *ISIS/Draw*, version 2.1; MDL Information Systems: San Diego, 1990−1996.
(53) Nagao, Y.; Hirata, T.; Goto, S.; Sano, S.; Kakehi, A.; Iizuka, K.; Shiro, M. Intramolecular Nonbonded S···O Interaction Recognized in (Acylimino)thiadiazoline Derivates as Angiotensin II Receptor Antagonists and Related Compounds. *J. Am. Chem. Soc.* **1998**, *120*, 3104−3110.

JM021032V